

# Féeton ( $B - L$ Gauge Boson) Dark Matter for the 511-keV Gamma-Ray Excess and the Prediction of Low-energy Neutrino Flux

Yu Cheng,<sup>1,2,\*</sup> Weikang Lin,<sup>3,1,2,†</sup> Jie Sheng,<sup>1,2,‡</sup> and Tsutomu T. Yanagida<sup>1,2,4,§</sup>

<sup>1</sup>*Tsung-Dao Lee Institute & School of Physics and Astronomy, Shanghai Jiao Tong University, China*

<sup>2</sup>*Key Laboratory for Particle Astrophysics and Cosmology (MOE)*

*& Shanghai Key Laboratory for Particle Physics and Cosmology, Shanghai Jiao Tong University, Shanghai 200240, China*

<sup>3</sup>*South-Western Institute For Astronomy Research,*

*Yunnan University, Kunming 650500, Yunnan, P. R. China*

<sup>4</sup>*Kavli IPMU (WPI), UTIAS, University of Tokyo, Kashiwa, 277-8583, Japan*

The féeton is the gauge boson of the  $U(1)_{B-L}$  gauge theory. If the gauge coupling constant is extremely small, it becomes a candidate for dark matter. We show that its decay to a pair of electron and positron explains the observed Galactic 511-keV gamma-ray excess in a consistent manner. This féeton dark matter decays mainly into pairs of neutrino and anti-neutrino. Future low-energy experiments with improved directional capability make it possible to capture those neutrino signals. The seesaw-motivated parameter space predicts a relatively short féeton lifetime comparable to the current cosmological constraint.

## I. INTRODUCTION

The heavy Majorana right-handed neutrinos are very attractive since they naturally induce tiny neutrino masses by the seesaw mechanism [1–4], and at the same time their decays in the early universe generate the Universe’s baryon asymmetry through the leptogenesis [5]. It is well known that all gauge anomalies involving the  $U(1)_{B-L}$  symmetry [4] are canceled out if we introduce three right-handed neutrinos in the standard model (SM). Therefore, it is very interesting to consider the gauge  $U(1)_{B-L}$  extension of the SM as the next step beyond the SM.

It has been pointed out that the  $B - L$  gauge boson can be identified with the dark matter (DM) if the  $B - L$  gauge coupling constant  $g_{B-L}$  is sufficiently small [6–8]. We call it the “féeton” or “féeton DM” [8].

Two of the present authors (W.L. and T.T.Y.) have recently shown [9] that the 511 keV gamma-ray excess from the center of our galaxy [10–12] can be explained by decay of the féeton to a pair of electron and positron. It successfully explains the upper bound of the positron injection energy that is inferred from the non-detection of the 1-3 MeV diffused gamma ray [13]. However, there are several caveats in such a scenario. First, in order to avoid an overproduction of electron-positron pairs, féeton can only constitute a small fraction of DM. Second, being a small fraction of DM means that it is much more difficult to search for the signal of neutrinos decayed from féeton DM. Third, it suffers from a mild tension that the resultant positron-annihilation flux is insufficiently sharp towards the Galactic center (GC), which is a common

issue for all proposals with DM decays [14].<sup>1</sup>

In this paper, we consider a new scenario for forming the positronium that allows féeton to be the dominant DM and significantly enhances the detectability. This new scenario predicts the neutrino flux of its energy peak at 511 keV with no higher-energy continuum. We discuss how to test this neutrino with low-energy neutrino experiments like Borexino and Juno.

## II. A NEW SCENARIO FOR THE 511 KEV GAMMA-RAY EXCESS AND CONSISTENT PARAMETERS IN THE FÉETON DM MODEL

In this section, we discuss a new parameter region of the original féeton DM model [8]. The low-energy physics is described by only two free parameters, the mass  $m_f$  and the gauge coupling constant  $g_{B-L}$  of the féeton. These two parameters are related by  $m_f = 2g_{B-L}V_{B-L}$ , where  $V_{B-L}$  is the Vacuum Expectation Value (VEV) of a Higgs boson  $\Phi$  with a  $B - L$  charge of +2. Here, the right-handed neutrinos,  $N_i$  ( $i = 1 - 3$ ), acquire Majorana masses of  $h_i V_{B-L}$  with the constant parameters  $h_i$  defined by the Yukawa interactions  $\frac{1}{2}h_i\Phi N_i N_i$ . We have assumed all leptons including the right-handed neutrinos have the  $B - L$  charge of  $-1$ .<sup>2</sup>

<sup>1</sup> However, the tension in the morphology of the signal between the observation and the prediction of DM decays is not decisive. There exist uncertainties in the transportation of positrons in the interstellar medium and more complete surveys in the disk area are still needed.

<sup>2</sup> The definition of  $B - L$  charge has an ambiguity related to the  $U(1)$  hypercharge gauge transformation [7]. However, our main conclusions are not much changed except for a very special parameter region where the féeton coupling to the electron and positron pair is suppressed [15].

\* [chengyu@sjtu.edu.cn](mailto:chengyu@sjtu.edu.cn)

† [weikanglin@ynu.edu.cn](mailto:weikanglin@ynu.edu.cn)

‡ [shengjie04@sjtu.edu.cn](mailto:shengjie04@sjtu.edu.cn)

§ [tsutomu.yanagida@sjtu.edu.cn](mailto:tsutomu.yanagida@sjtu.edu.cn)

The decay rate  $\Gamma_f$  of the féeton is given by

$$\Gamma_f = \frac{g_{B-L}^2 m_f}{24\pi} \left[ 3 + 2\sqrt{1 - \frac{4m_e^2}{m_f^2}} \left( 1 + \frac{2m_e^2}{m_f^2} \right) \right], \quad (1)$$

where we assume  $m_f > 2m_e$  so that both the decays to the neutrino-anti-neutrino pairs and the electron-positron pair are included,  $m_e$  is the electron mass and the neutrino masses have been ignored. Then, we see the reason why the féeton cannot be the dominant DM. The electron-positron pairs would be over-produced and the resultant Galactic 511 keV gamma ray would largely exceed the observation as long as the branching ratio of the  $f \rightarrow e + \bar{e}$  decay channel is  $O(1)$  as pointed out in [9].

Now we are at the main point of this paper. If the féeton mass  $m_f$  is very close to the threshold of the decay to the electron-positron pair, that is,  $m_f \simeq 2m_e$ , such a decay is strongly suppressed and the branching ratio to the  $e + \bar{e}$  final state becomes very small so that the predicted excess of the 511 keV gamma ray can be consistent with the observation while the féeton is the dominant DM. However, it does not look successful. It is usually assumed that the intermediate state of positronium is formed by the produced positrons by charge exchanges with neutral hydrogen atoms [13]. This can happen only if the kinetic energy of the positron is larger than the corresponding threshold 6.8 eV—the difference in the binding energy between neutral hydrogen and positronium. This sets the lower bound of the féeton mass and hence the  $e + \bar{e}$  branching ratio.

However, if the produced positrons have a kinetic energy smaller than 6.8 eV, instead of with neutral hydrogen atoms, they can predominantly form positronium with free electrons in warm or hot ionized gas; see, e.g., Fig. 27 in [13]. This possibility has been largely overlooked in the literature. Thus, we consider the following scenario. The féeton constitutes the total DM and has a mass very close to the threshold of the decay to an electron-positron pair, more explicitly,  $2m_e < m_f < 2m_e + 13.6$  eV. They decay to electrons and positrons with a small branching ratio compared to the decay to neutrinos and anti-neutrinos. The produced positrons mainly form positroniums with free electrons in ionized environments, which subsequently annihilate to produce the 511 keV gamma rays.

Assuming there are sufficient free electrons so that the positron produced from féeton decays annihilate immediately and the gamma-ray emission rate traces the féeton decay rate. The angular differential gamma-ray flux is given in [9]. In the first order of  $\Delta m/m_e$ , it reads,

$$\frac{d\Phi_{511}}{d\Omega} = 4 \times 10^3 \left( \frac{g_{B-L}}{10^{-20}} \right)^2 \left( \frac{\Delta m}{m_e} \right)^{1/2} \times \tilde{D}_N(\cos\theta) [\text{cm}^{-2}\text{s}^{-1}\text{sr}^{-1}], \quad (2)$$

where  $\Delta m \equiv m_f - 2m_e$ ,  $\tilde{D}_N(\cos\theta)$  is a function that represents the morphology of the flux and is normalized

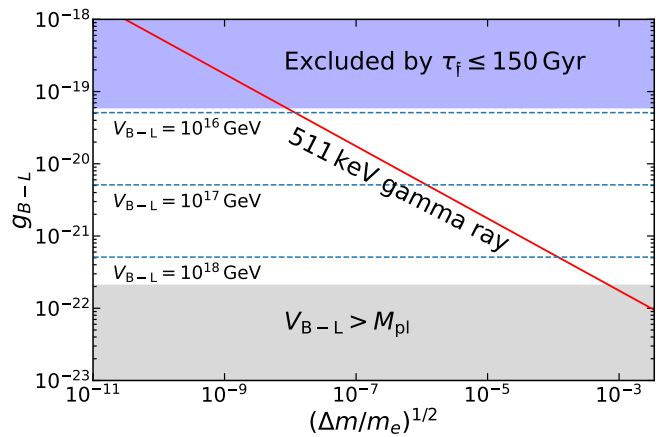


FIG. 1. The red line shows the corresponding  $g_{B-L}$  to explain the observed 511 keV gamma ray excess. The blue-shaded region is excluded by supposing the lifetime of féeton should be larger than ten times of the universe age,  $\tau_f > 150$  Gyr. The gray-shaded region represents for  $V_{B-L} > M_{\text{pl}} = 2.4 \times 10^{18}$  GeV.

so that  $\int \tilde{D}_N d\Omega = 4\pi$ . The angle between the direction of the flux and GC  $\theta$  is defined by  $\cos\theta \equiv \cos b \cos \ell$  with galactic coordinates  $(b, \ell)$ . The morphology function  $\tilde{D}_N(\cos\theta)$  depends on the Galactic DM distribution which we have adopted an NFW profile [16].

Recall that Ref. [17] measures a 511-keV gamma-ray intensity of  $0.96 \pm 0.07 \text{ cm}^{-2} \text{ s}^{-1}$  from the bulge region with a Full-Width-at-Half-Magnitude (FWHM) of 20.55 degrees. To proceed, we integrate (2) within  $\theta < 10.28$  degrees from GC and set it as half of the measured bulge flux to be the observed bulge 511-keV gamma-ray intensity. This gives us the féeton DM parameter space that can explain the observed 511-keV gamma ray, which is shown as the red line in Fig. 1. We also show the parameter space excluded by the lifetime constraint (purple) and that with a super-Planckian VEV (gray). As expected, the féeton mass should be close to twice the electron mass. The closer  $m_f$  to  $2m_e$ , the larger the gauge coupling constant should be to account for the 511 keV gamma ray intensity. For the maximally allowed gauge coupling constant, i.e.,  $g_{B-L} \simeq 6 \times 10^{-20}$ , we require  $(\Delta m/m_e)^{1/2} \simeq 10^{-8}$ . The mass difference  $\Delta m$  is identified to be the total kinetic energy of the electron-positron pair produced by the féeton decay and thus the positrons are non-relativistic<sup>3</sup>.

The above has demonstrated that the féeton can constitute the total DM while being able to explain the intensity of the 511-keV gamma ray considering that the non-

<sup>3</sup> An alternative way to suppress the féeton decay to the electron and positron is given by the mechanism mentioned in footnote 2. In this case, it might be interesting that the anti-neutrinos produced from the féeton decay causes the 511 keV gamma ray emissions in the detector. However, it will be not easy to distinguish the signal from the geo neutrinos.

relativistic positrons produced from féeton decays form positronium with free electrons in ionized environments. Since now the féeton is not merely a tiny fraction of DM, it significantly enhances the neutrino and anti-neutrino fluxes produced from féeton decays as compared to the scenario in the previous work [9]. In addition, the neutrino and anti-neutrino energies peak at 511 keV, which is above the threshold for directional determination by current detectors that use Cherenkov lights. Thus, the new scenario in this work has much better detectability compared to that in [8].

### III. POSSIBLE DETECTION OF THE PREDICTED NEUTRINOS AT THE LOW-ENERGY NEUTRINO EXPERIMENTS

#### A. Low-energy neutrino detectors

The main decay mode of the féeton is that to the neutrino-anti-neutrino pair. The energy of the resultant neutrinos is peaked at  $\simeq 511$  keV because the féeton mass is just above the threshold of the decay, that is,  $m_f \simeq 2m_e$  as explained in the previous section. The neutrino flux from the Galactic and the extra-galactic féeton DM decay have been calculated in [8]. In this section, we discuss the detectability of the corresponding neutrino flux by setting the féeton mass to  $\simeq 1$  MeV and taking the optimal coupling constant allowed by the DM lifetime constraint, i.e.,  $g_{B-L} = 5.85 \times 10^{-20}$ ; see Ref.[8]. This value of  $g_{B-L}$  is also the most motivated value as we shall explain.

We first discuss the detectability for solar neutrino experiments since the predicted energy falls into their target energy range. Adopting Eq. (5) in [8] with  $g_{B-L} = 5.85 \times 10^{-20}$ , we see that the neutrino flux of the féeton decay is  $\simeq 3.4 \times 10^6 \text{ cm}^{-2}\text{s}^{-1}$ , which is three-order-of-magnitude smaller than the  ${}^7\text{Be}$  neutrino flux [18] although the peak energy is different. We then evaluate the electron recoil spectrum per unit mass of liquid scintillator as the neutrinos from the féeton decay scatter off electrons in neutrino detectors. The energy differential event count is,

$$\frac{dN}{dE_e} = \int dE_\nu \frac{d\Phi_\nu}{dE_\nu} \cdot \frac{d\sigma}{dE_e}(E_\nu) \cdot N_T \cdot t. \quad (3)$$

Here,  $E_e$  is the kinetic energy of the recoil electron,  $\frac{d\Phi_\nu}{dE_\nu}$  is the neutrino flux from the féeton decay [8, 9],  $N_T = (3.307 \pm 0.015) \times 10^{29}$  is the number of electrons per ton of the liquid scintillator [19],  $t$  is the exposure time which we take one year for illustration. Besides, the neutrino-electron scattering differential cross section is given by

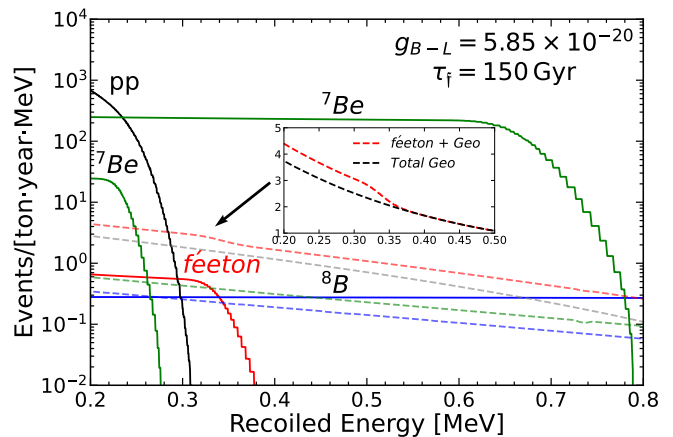


FIG. 2. Electron recoil energy spectra caused by different neutrino sources. The red line shows the electron recoil spectrum for maximum neutrino flux from féeton decay by assuming  $\tau_f = 150$  Gyr which corresponds to  $g_{B-L} = 5.85 \times 10^{-20}$ . The electron recoil spectrum from the solar  $pp$  ( ${}^7\text{Be}$ ,  ${}^8\text{B}$ ) is shown as the black (green, blue) line. The geo-neutrino contribution from K (U, Th) decay is shown as a gray (green, blue) dashed line. The red-dashed curve shows the spectrum for the total geo-neutrinos plus the féeton neutrinos. For comparison, the total geo-neutrinos background is shown as the black dashed line in the subfigure.

[20],

$$\frac{d\sigma}{dE_e} = \frac{G_F^2 m_e}{2\pi} \left[ (g_V + g_A)^2 + (g_V - g_A)^2 \left(1 - \frac{E_e}{E_\nu}\right)^2 - (g_V^2 - g_A^2) \frac{m_e E_e}{E_\nu^2} \right]. \quad (4)$$

For the electric neutrino-electron scattering,  $g_V = 1/2 + 2e^2/g^2$  and  $g_A = 1/2$ . For the  $\nu_\mu$ - and  $\nu_\tau$ -electron scatterings,  $g_V = (-1/2 + 2e^2/g^2)$ ,  $g_A = -1/2$  where  $g$  is the weak gauge coupling. For the anti-neutrino electron scatterings, the corresponding cross sections can be obtained by replacing  $g_A$  with  $-g_A$  in Eq. (4).

The resultant electron recoil spectrum caused by the neutrino flux from the féeton decay is shown by the red line in Fig. 2, along with those for the solar neutrinos of different channels. We can see the spectrum for the féeton case is of the same order as that of  ${}^8\text{B}$  and almost three-order-of-magnitude smaller than  ${}^7\text{Be}$ .

The most serious problem, however, is the presence of several isotope decays inside the scintillators in low-energy solar neutrino experiments such as Borexino. For example, the beta decay of  ${}^{210}\text{Po}$  produces neutrinos whose energy range covers 511 keV and flux is 7 ~ 8 order magnitude larger than the féeton neutrino flux [21, 22]. Removing such contamination is crucial for the search of the féeton neutrino flux. In this paper we will not discuss the purification mechanism [23] of such isotopes and only assume that we can remove such background neutrinos at a sufficient level for the detection of the féeton neutri-

nos and discuss possible discrimination of féeton signals from the solar neutrinos, mainly  ${}^7\text{Be}$  neutrinos.

Another problem is the geo-neutrino contamination. Geo-neutrinos consist of electron-type anti-neutrinos produced by the beta decay of radionuclides, mostly  ${}^{40}\text{K}$ ,  ${}^{232}\text{Th}$ , and  ${}^{235}\text{U}$ , in the Earth [24]. Their energies range from 0.1 MeV to 3 MeV. As the dashed lines shown in Fig. 2, the geo-neutrino contributions for the electron recoils are larger than that for the féeton neutrino. However, it is still possible for a Borexino-type experiment to distinguish it through direction information.

To mitigate the problems from the solar neutrinos and geo-neutrinos, one may utilize the direction dependence and the time modulation of neutrino fluxes. The solar neutrino flux comes from the sun and our féeton neutrino flux is more concentrated towards GC. Fig. 3 shows the angular dependence of the féeton neutrino flux assuming the féeton DM distribution follows an NFW profile [16] in our galaxy, where  $\theta$  is the angle between the line of sight and GC. The féeton neutrino flux from GC is the most intense and thus allows the highest directionality. In Fig. 3 we also include the uniform neutrino flux decayed from the extragalactic féeton DM.

Some recent solar neutrino detectors already equip direction determination capability. For instance, the Borexino experiment combines both the water Cherenkov and liquid scintillator detectors, it gathers the first directional measurement of sub-MeV solar neutrinos [25]. Light signals are produced via neutrinos scattering off electrons. For water Cherenkov detectors, if the recoil electron moves faster than the speed of light in water, the directional Cherenkov light is produced. Since the speed of light in water is around  $v_c \simeq 0.75c$ , the kinetic energy of the recoil electron should be larger than  $E_e \simeq 0.5m_e$  to produce Cherenkov lights. The corresponding minimum energy of the neutrino is 420 keV. Thus, the energy of the féeton neutrinos is above the threshold, which allows us to make direction determination via water Cherenkov detectors. On the other hand, an electron with a kinetic energy of  $0.5m_e$  is relativistic. Such a large recoil energy can only be produced by an almost-forward scattering by a 511-keV neutrino. Therefore, for the féeton neutrino case, the direction of the recoil electron almost tracks the direction of the incoming neutrino.

Since the Earth is orbiting the sun, the direction of the sun is changing while the direction of GC is not. The sun and galaxy center have nearly opposite directions related to the Earth around June, which makes féeton neutrino flux the most distinguishable from the solar neutrinos in terms of direction. Similarly, geo-neutrinos only come from the inside of the Earth. Based on the GC location around June, a detector should be put in the south hemisphere so that the geo-neutrinos and the féeton neutrinos from the GC region are in opposite directions.

The above discusses the difference in the direction of each signal. However, the geo-neutrinos are much more diffuse than the solar neutrinos and are more difficult to get rid of using direction determination. Fortunately, the

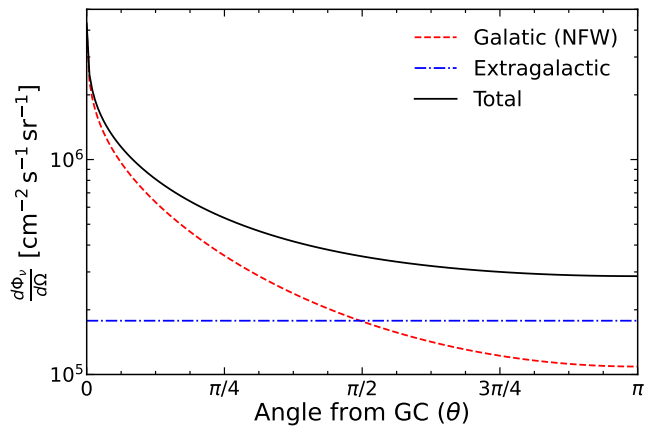


FIG. 3. The angle distribution for neutrino flux from féeton DM decay with mass  $m_f \simeq 2m_e$  and coupling  $g_{B-L} = 5.85 \times 10^{-20}$ . The red dashed line shows the Galactic contribution with NFW profile and the blue dash-dotted line shows the extra-galactic contribution. Their combination is the black solid curve.

total geo-neutrino intensity is only several times larger than that of the féeton neutrinos. Suppose the solar neutrino signal can be sufficiently identified and subtracted using direction determination, we obtain the electron recoil spectrum for the total geo-neutrinos and féeton neutrinos which we show by the red-dashed curve in Fig. 3. We can see a characteristic kink at  $\sim 0.35$  MeV. This feature at that specific energy is so far unique for all known neutrino sources. While there is some uncertainty in the geo-neutrino intensity, this feature persists in the otherwise smooth geo-neutrino electron-recoil spectrum as long as the 511-keV féeton neutrinos exist. Detecting such a kink will be a smoking gun to the 511-keV neutrinos and the féeton DM.

## B. Cosmological probes

Taking  $m_f \simeq 2m_e$ , the DM lifetime constraint sets an upper bound of  $g_{B-L} \lesssim 6 \times 10^{-20}$  as explained in Ref. [8]. On the other hand, we still have a large parameter space on the lower bound of the gauge coupling constant  $g_{B-L}$ , which is determined by the upper bound of the  $B-L$  breaking scale. Provided a conservative upper bound  $V_{B-L} < M_{Pl}$  where  $M_{Pl} \simeq 2.4 \times 10^{18}$  GeV is the reduced Planck mass, we have  $g_{B-L} \gtrsim 2 \times 10^{-22}$  using  $m_f = 2g_{B-L}V_{B-L}$  and  $m_f \simeq 2m_e$ .

However, not all of the parameter space between  $6 \times 10^{-22} \lesssim g_{B-L} \lesssim 2 \times 10^{-20}$  is equally motivated. It is remarkable that the observed neutrino mass  $m_\nu \simeq 0.05$  eV naturally predicts the  $B-L$  breaking scale  $V_{B-L}$  to be  $O(10^{16})$  GeV [26] provided that all the Yukawa coupling constants for the third family right-handed neutrino  $N_3$  such as  $h_3$  are  $O(1)$ . Taking that  $V_{B-L} \simeq 10^{16}$  GeV and that  $m_f \simeq 2m_e$  required to explain the Galactic 511 keV gamma-ray excess, we have  $g_{B-L} \simeq 5 \times 10^{-20}$ . Thus, the

value of  $g_{B-L}$  we took in Sec. III A is not merely an optimal coupling constant, but also a very motivated one. More importantly, with these values of  $g_{B-L}$  and  $m_f$ , we predict that the féeton DM lifetime to be  $\sim 150$  Gyr. This is very encouraging because it is already close to the cosmological constraint on the DM lifetime obtained with the cosmic background and large-scale-structure (LSS) probes [27–30]. Therefore, the féeton DM scenario proposed in this work implies that the cosmological effects due to the féeton DM decay can soon be detected via cosmological probes with the near-future galaxy surveys such as LSST<sup>4</sup>, DESI<sup>5</sup>, Euclid<sup>6</sup> and WFIRST<sup>7</sup>, and the on-going mission JWST<sup>8</sup>.

#### IV. DISCUSSION AND CONCLUSIONS

In this paper, we have shown a scenario in which the féeton is the dominant DM and consistently explains the observed magnitude of the Galactic 511-keV gamma-ray excess by the féeton DM decay into electron and positron. The scenario pins down the mass of the féeton very close to  $2m_e$  so that the electron and positron produced by the féeton decay are highly non-relativistic. The injection kinetic energy of the positrons is less than 13.6 eV so that they do not form positronium via charge exchanges with neutral hydrogen atoms, which is usually taken in the literature. Rather, we consider that they form positronium with free electrons in ionized environments. Different from the previous cases [8, 9], the scenario in this work produces larger neutrino and anti-neutrino fluxes with an energy that is high enough for direction determination with the current solar neutrino experiments. In the future, solar neutrino experiments with improved angular resolution are promising to detect the neutrinos decayed from the féeton DM. The parameter space that is consistent with the high-scale Seesaw mechanism also predicts that the féeton lifetime is close to the current cosmological constraint. Thus, it implies the effects on the cosmic background evolution and LSS should be soon detected via near-future galaxy surveys.

Since the produced positrons are highly non-relativistic, it implies there is no higher-energy continuum in the gamma-ray excess that would be produced as high-energy positrons fly through the Galactic medium. This provides another crucial test of the scenario. Future experiments, such as the Compton Spectrometer and Image (COSI) mission that aims at detecting the soft gamma-ray of  $0.2 \sim 5$  MeV [31] will give us strong constraints on the present féeton DM model.

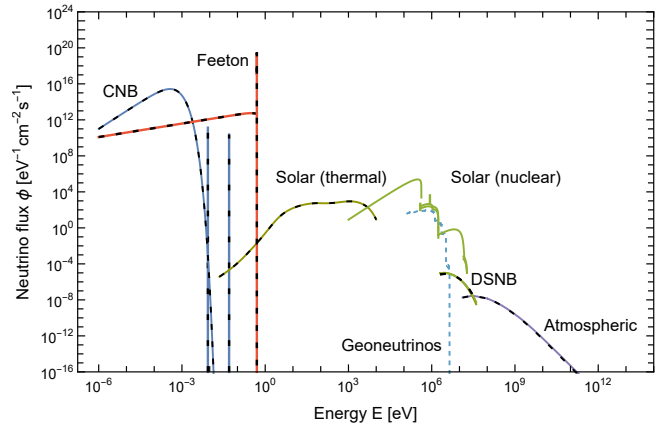


FIG. 4. The energy spectra of neutrino flux from different sources with different colors [24]. Solid lines represent for neutrino flux while dashed lines for anti-neutrino. Among them, the red lines show the neutrino flux from féeton decay with taking féeton mass to be  $m_f = 1$  eV. The galactic signal is a delta-line spectrum with total flux  $3.5 \times 10^{12} \text{ cm}^{-2} \text{ s}^{-1}$  while the continuous spectrum corresponds to the extra-galactic signal.

It is assumed in this work that féeton is the dominant component of the DM in the present Universe. Normally, it seems very difficult to produce the féeton in the early Universe, since its gauge coupling constant  $g_{B-L}$  is extremely small. However, it is pointed out that the light gauge bosons  $\mathcal{V}$  can be produced abundantly during the inflation independent of the magnitude of their gauge coupling constant. In fact, the abundance  $\Omega_{\mathcal{V}}$  is given by [32],

$$\Omega_{\mathcal{V}} \simeq 0.3 \left( \frac{m_{\mathcal{V}}}{6 \times 10^{-6} \text{ eV}} \right)^{1/2} \left( \frac{H_{\text{inf}}}{10^{14} \text{ GeV}} \right)^2, \quad (5)$$

where  $m_{\mathcal{V}}$  and  $H_{\text{inf}}$  are the mass of the gauge boson and the Hubble constant during inflation, respectively. With a féeton mass  $m_f \simeq 1$  MeV and setting  $\Omega_{\mathcal{V}} = \Omega_f \simeq 0.25$ , we predict  $H_{\text{inf}} \simeq 1.6 \times 10^{11} \text{ GeV}$ , which is a rather low-energy inflation. Recall that  $H_{\text{inf}} \simeq 2.6 r^{1/2} \times 10^{14} \text{ GeV}$  assuming a slow-roll inflation [33], where  $r$  is the primordial tensor-to-scalar ratio. The ratio  $r$  is then predicted to be very low, i.e.,  $r \simeq 4 \times 10^{-7}$ . Thus, if the next-generation Cosmic Microwave Background (CMB) experiments detected the primordial B-mode polarization, the above féeton DM production scenario would be falsified and either the féeton was not the dominant DM or it was produced by other mechanisms [34].

Finally, we would give a general comment on the féeton DM hypothesis. Figure 4 shows different neutrino fluxes from the known sources in increasing order of energy [24]. It contains from the cosmic neutrino background (CNB) of  $10^{-6}$  eV to the atmospheric neutrino of  $10^{12}$  eV. However, there is a blank between 0.1 eV and 1 keV. Although different from the scenario proposed in this work, it would be interesting for the féeton neutrino to be a candidate to

<sup>4</sup> <http://www.lsst.org/lsst>.

<sup>5</sup> <https://www.desi.lbl.gov/>.

<sup>6</sup> <http://sci.esa.int/euclid>.

<sup>7</sup> <https://www.skatelescope.org>.

<sup>8</sup> <https://webb.nasa.gov>.

fill the blank if the féeton mass is  $m_f = 0.1 \text{ eV} \sim 1 \text{ keV}$ , which can be achieved with a low-energy Seesaw mechanism. Taking  $m_f = 1 \text{ eV}$  for example, the neutrino contribution from the féeton decay is shown as the red solid curve in Fig. 4, while the anti-neutrino contribution with the same flux is shown as the dashed curve. An interesting search for the féeton neutrino is given by the measurement of anti-neutrinos. An example has been proposed for the measurement of the cosmic anti-neutrino [35, 36]. It uses the capture of the electron-type anti-neutrino on the  $^{163}\text{Ho}$  atom,



where  $E_i$  is some binding energy from the de-excitation of the Dy atom. Based on the red dashed curve in Fig. 4, the integrated anti-neutrino flux from féeton decay with

$m_f \sim 1 \text{ eV}$  is larger than that of CNB. This means the capture rate of the féeton anti-neutrino on  $^{163}\text{Ho}$  is larger than the capture rate of the cosmic anti-neutrino. So the low-mass féeton can be tested in such experiments.

## ACKNOWLEDGMENTS

T. T. Y. thanks Shigeki Matsumoto for the discussion on the possible suppression of the electron-positron coupling of the féeton. T. T. Y. is supported in part by the China Grant for Talent Scientific Start-Up Project and by Natural Science Foundation of China (NSFC) under grant No. 12175134 as well as by World Premier International Research Center Initiative (WPI Initiative), MEXT, Japan.

- 
- [1] P. Minkowski, “ $\mu \rightarrow e\gamma$  at a Rate of One Out of  $10^9$  Muon Decays?,” *Phys. Lett.* **67B** (1977) 421–428.
- [2] T. Yanagida, “Horizontal gauge symmetry and masses of neutrinos,” *Proceedings: Workshop on the Unified Theories and the Baryon Number in the Universe: KEK, Japan, February 13-14, 1979, Conf. Proc. C7902131* (1979) 95–99.  
T. Yanagida, “Horizontal Symmetry and Mass of the Top Quark,” *Phys. Rev. D* **20** (1979) 2986.
- [3] M. Gell-Mann, P. Ramond, and R. Slansky, “Complex Spinors and Unified Theories,” *Conf. Proc. C790927* (1979) 315–321, [arXiv:1306.4669 [hep-th]].
- [4] F. Wilczek *Proceedings: Lepton-Photon Conference (Fermilab, Aug 1979) Conf. Proc. C790885* (1979) .
- [5] M. Fukugita and T. Yanagida, “Baryogenesis Without Grand Unification,” *Phys. Lett. B* **174** (1986) 45–47.
- [6] G. Choi, T. T. Yanagida, and N. Yokozaki, “Feebly interacting  $U(1)_{B-L}$  gauge boson warm dark matter and XENON1T anomaly,” *Phys. Lett. B* **810** (2020) 135836, [arXiv:2007.04278 [hep-ph]].
- [7] N. Okada, S. Okada, D. Raut, and Q. Shafi, “Dark matter  $Z'$  and XENON1T excess from  $U(1)_X$  extended standard model,” *Phys. Lett. B* **810** (2020) 135785, [arXiv:2007.02898 [hep-ph]].
- [8] W. Lin, L. Visinelli, D. Xu, and T. T. Yanagida, “Neutrino astronomy as a probe of physics beyond the Standard Model: decay of sub-MeV  $B-L$  gauge boson dark matter,” [arXiv:2202.04496 [hep-ph]].
- [9] W. Lin and T. T. Yanagida, “Confronting the Galactic 511 keV emission with  $B-L$  gauge boson dark matter,” *Phys. Rev. D* **106** no. 7, (2022) 075012, [arXiv:2205.08171 [hep-ph]].
- [10] I. Johnson, W. N., J. Harnden, F. R., and R. C. Haymes, “The Spectrum of Low-Energy Gamma Radiation from the Galactic-Center Region.,” *ApJ* **172** (Feb., 1972) L1.
- [11] R. C. Haymes, G. D. Walraven, C. A. Meegan, R. D. Hall, F. T. Djuth, and D. H. Shelton, “Detection of nuclear gamma rays from the galactic center region.,” *ApJ* **201** (Nov., 1975) 593–602.
- [12] M. Leventhal, C. J. MacCallum, and P. D. Stang, “Detection of 511 keV positron annihilation radiation from the galactic center direction.,” *ApJ* **225** (Oct., 1978) L11–L14.
- [13] J. F. Beacom and H. Yuksel, “Stringent constraint on galactic positron production,” *Phys. Rev. Lett.* **97** (2006) 071102, [arXiv:astro-ph/0512411].
- [14] Y. Ascasibar, P. Jean, C. Boehm, and J. Knödseder, “Constraints on dark matter and the shape of the Milky Way dark halo from the 511-keV line,” *Monthly Notices of the Royal Astronomical Society* **368** no. 4, (04, 2006) 1695–1705.
- [15] H. Fukuda, S. Matsumoto, and T. Yanagida, *unpublished discussion* (2024) .
- [16] J. F. Navarro, C. S. Frenk, and S. D. M. White, “The Structure of cold dark matter halos,” *Astrophys. J.* **462** (1996) 563–575, [arXiv:astro-ph/9508025].
- [17] T. Siebert, R. Diehl, G. Khachatryan, M. G. H. Krause, F. Guglielmetti, J. Greiner, A. W. Strong, and X. Zhang, “Gamma-ray spectroscopy of Positron Annihilation in the Milky Way,” *Astron. Astrophys.* **586** (2016) A84, [arXiv:1512.00325 [astro-ph.HE]].
- [18] J. N. Bahcall and M. H. Pinsonneault, “What do we (not) know theoretically about solar neutrino fluxes?,” *Phys. Rev. Lett.* **92** (2004) 121301, [arXiv:astro-ph/0402114].
- [19] S. Kumaran, L. Ludhova, O. Penek, and G. Settanta, “Borexino Results on Neutrinos from the Sun and Earth,” *Universe* **7** no. 7, (2021) 231, [arXiv:2105.13858 [hep-ex]].
- [20] G. 't Hooft, “Predictions for neutrino - electron cross-sections in Weinberg’s model of weak interactions,” *Phys. Lett. B* **37** (1971) 195–196.
- [21] G. Bellini *et al.*, “Precision measurement of the  $7\text{Be}$  solar neutrino interaction rate in Borexino,” *Phys. Rev. Lett.* **107** (2011) 141302, [arXiv:1104.1816 [hep-ex]].
- [22] BOREXINO Collaboration, A. Pocar *et al.*, “Solar Neutrino Physics with Borexino,” *SciPost Phys. Proc.* **1** (2019) 025, [arXiv:1810.12967 [nucl-ex]].
- [23] G. Bellini, “The impact of Borexino on the solar and neutrino physics,” *Nucl. Phys. B* **908** (2016) 178–198.
- [24] E. Vitagliano, I. Tamborra, and G. Raffelt, “Grand

- Unified Neutrino Spectrum at Earth: Sources and Spectral Components*,” *Rev. Mod. Phys.* **92** (2020) 45006, [[arXiv:1910.11878](#) [astro-ph.HE]].
- [25] **BOREXINO** Collaboration, M. Agostini *et al.*, “Correlated and integrated directionality for sub-MeV solar neutrinos in Borexino,” *Phys. Rev. D* **105** no. 5, (2022) 052002, [[arXiv:2109.04770](#) [hep-ex]].
- [26] W. Buchmuller and T. Yanagida, “Quark lepton mass hierarchies and the baryon asymmetry,” *Phys. Lett. B* **445** (1999) 399–402, [[arXiv:hep-ph/9810308](#)].
- [27] S. De Lope Amigo, W. M.-Y. Cheung, Z. Huang, and S.-P. Ng, “Cosmological Constraints on Decaying Dark Matter,” *JCAP* **06** (2009) 005, [[arXiv:0812.4016](#) [hep-ph]].
- [28] B. Audren, J. Lesgourgues, G. Mangano, P. D. Serpico, and T. Tram, “Strongest model-independent bound on the lifetime of Dark Matter,” *JCAP* **12** (2014) 028, [[arXiv:1407.2418](#) [astro-ph.CO]].
- [29] **DES** Collaboration, A. Chen *et al.*, “Constraints on dark matter to dark radiation conversion in the late universe with DES-Y1 and external data,” *Phys. Rev. D* **103** no. 12, (2021) 123528, [[arXiv:2011.04606](#) [astro-ph.CO]].
- [30] K. Enqvist, S. Nadathur, T. Sekiguchi, and T. Takahashi, “Constraints on decaying dark matter from weak lensing and cluster counts,” *JCAP* **04** (2020) 015, [[arXiv:1906.09112](#) [astro-ph.CO]].
- [31] **COSI** Collaboration, J. A. Tomsick, “The Compton Spectrometer and Imager Project for MeV Astronomy,” *PoS ICRC2021* (2021) 652, [[arXiv:2109.10403](#) [astro-ph.IM]].
- [32] P. W. Graham, J. Mardon, and S. Rajendran, “Vector Dark Matter from Inflationary Fluctuations,” *Phys. Rev. D* **93** no. 10, (2016) 103520, [[arXiv:1504.02102](#) [hep-ph]].
- [33] **Planck** Collaboration, Y. Akrami *et al.*, “Planck 2018 results. X. Constraints on inflation,” *Astron. Astrophys.* **641** (2020) A10, [[arXiv:1807.06211](#) [astro-ph.CO]].
- [34] **CMB-S4** Collaboration, K. Abazajian *et al.*, “Snowmass 2021 CMB-S4 White Paper,” [[arXiv:2203.08024](#) [astro-ph.CO]].
- [35] M. Vignati and M. Lusignoli, “ $^{163}\text{Ho}$  as a target for cosmic antineutrinos,” *Journal of Physics: Conference Series* **375** no. 4, (Jul, 2012) 042006. <https://dx.doi.org/10.1088/1742-6596/375/1/042006>.
- [36] L. Gastaldo *et al.*, “The electron capture in  $^{163}\text{Ho}$  experiment – ECHO,” *Eur. Phys. J. ST* **226** no. 8, (2017) 1623–1694.